

# Comparing investigation for a Bi-directional Isolated DC/DC Converter using Series Voltage Compensation

Satoshi Miyawaki  
Nagaoka University of Technology  
Niigata, Japan  
miyawaki@stn.nagaokaut.ac.jp

Jun-ichi Itoh  
Nagaoka University of Technology  
Niigata, Japan  
itoh@vos.nagaokaut.ac.jp

Kazuki Iwaya  
TDK-LAMBDA, Ltd  
Niigata, Japan  
k.iwaya@jp.tdk-lambda.com

**Abstract** -- This paper discusses a bi-directional isolated DC/DC converter using series compensation method. The proposed converter consists of a high efficiency resonance full-bridge converter and a series converter. This proposed circuit regulates the output voltage by the series converter, which provides only the differential voltage between the input voltage and the output voltage, which is closed to the nominal voltage. In this paper, four types of the auxiliary circuits are investigated in term of loss. The relationship between the loss element and efficiency characteristics is clarified. The validity of the proposed circuit is confirmed by the loss calculation, with a maximum efficiency of over 94% at 2kW. Moreover, the experimental results confirmed that the proposed circuit, which converts 48-V to 380-V at 1kW, achieves the maximum efficiency of 93.0% at the nominal input voltage region.

## I. INTRODUCTION

Recently, high efficiency and high power density for the bi-directional isolated DC/DC converters are increasingly desired for smart grid system. The applications of the DC/DC converters are such as the secondary battery conversion and power conditioner for photovoltaic cell or fuel cell. In addition, these power converters have to control a wide range of output voltage [1-9].

Current resonant type full-bridge converters, which use the resonance between the leakage inductance of transformers and the resonant capacitor, are one of the most effective circuit topologies to obtain high efficiency. However, it is difficult to regulate the output voltage in a wide range while there is a fluctuation in the input voltage because the switching timing is constrained by the resonance period. Therefore, a current resonant type full-bridge converter is generally connected to a voltage control converter, such as a buck chopper [10-11]. As a result, the converter loss will increase because all the power passes through two converters.

This paper proposes a new topology for a bi-directional isolated DC/DC converter using the series voltage compensation [12]. The input voltage fluctuation is compensated by the auxiliary circuit that outputs only the fluctuation of the output voltage. One of the advantages of the proposed circuit is that high efficiency can be achieved when

the input voltage is closed to the nominal input voltage because the power of the auxiliary circuit becomes very small in comparison to the input power. Normally, the large fluctuations occur in the input or output voltage is for certain short periods, and as a result, the converter loss can be reduced.

This paper discusses and evaluates the losses of the proposed circuit. In order to achieve the high efficiency, four types of the auxiliary circuits are investigated and it is necessary to clarify the optimization design procedure in terms of the efficiency characteristics. The mathematical expression is first established to estimate the power loss. The point of the mathematical expression is to observe the losses of a converter based on the study of device conditions. The first section of this paper introduces the principle of the proposed series compensation method. Secondary, mathematical expression is established in order to estimate the power loss. Thirdly, the proposed calculation method to evaluate the power loss is confirmed with the experimental results. Finally, some experimental results are given in order to demonstrate the advantages of the proposed converter.

## II. CIRCUIT CONFIGURATIONS

### A. Conventional Circuit

Fig. 1 shows the power flow diagram of the conventional converter. The conventional converter consists of a resonant converter and the voltage control converter, such as a chopper circuit. The fluctuation of the input voltage is constantly controlled by the chopper. The output side is isolated by the resonant converter. This system has two stages of power flow from the input to the output. The total efficiency of the conventional circuit  $\eta_c$  is obtained from (1), using both the resonant converter efficiency  $\eta_r$  and the buck chopper efficiency  $\eta_{chop}$ .

$$\eta_c = \eta_r \eta_{chop} \quad (1)$$

As a result, all the power passes through both converters despite of the relation with the input voltages; therefore, the converter efficiency is reduced.

### B. Proposed Circuit

Fig. 2 shows the power flow diagram of the proposed converter. In the proposed circuit, the resonant converter is used in the main circuit for the voltage isolation. In order to obtain the maximum efficiency, the resonant converter operates at a constant duty cycle based on the resonance frequency  $f_0$ . Then, the auxiliary circuit is used to regulate the output voltage. The output voltage of the auxiliary circuit is added to the output of the main circuit by a transformer. That is, the auxiliary circuit compensates only the fluctuation voltage, against the output voltage commands.

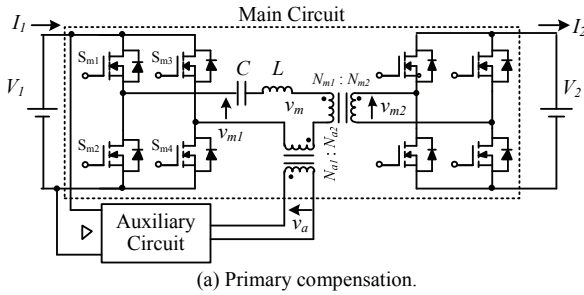
The proposed system consists of two power converters, which are connected in series to the output side. The following explains the proposed circuit can achieve high efficiency. The power  $P_{out}$  is obtained by adding the auxiliary converter power  $P_a$  to the directly power  $P_r$ . The total converter efficiency of the proposed circuit  $\eta_p$  is obtained by (2), using the auxiliary circuit efficiency  $\eta_a$  and the power ratio  $k=P_a/P_r$ .

$$\eta_p = \frac{\eta_r + k\eta_a}{1+k} \quad (2)$$

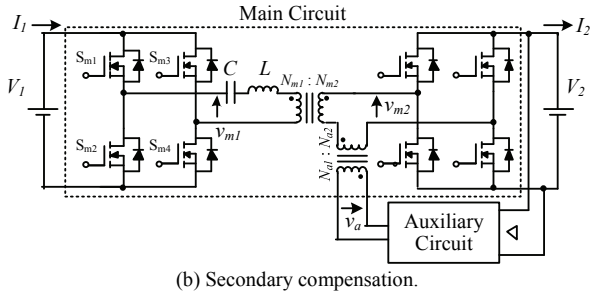
Therefore, the total efficiency  $\eta_p$  of the proposed circuit is higher than the conventional circuit where the efficiency can be expressed by (3).

$$\frac{\eta_r + k\eta_a}{1+k} > \eta_r \eta_{chop} \quad (3)$$

Fig. 3 shows the proposed circuit using the series voltage compensation. The main circuit is controlled under an optimum condition similar to the resonant converter. In order to obtain the maximum efficiency, the resonant converter operates at 50% duty cycle based on the resonance frequency  $f_0$ . Therefore, the main circuit can achieve zero current switching (ZCS) at any time. The resonance frequency of the

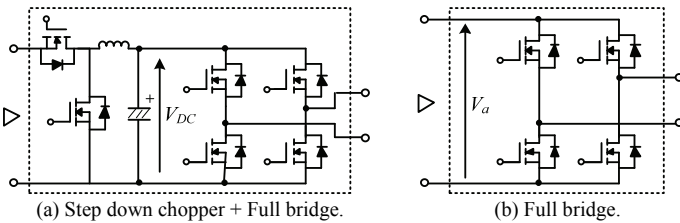


(a) Primary compensation.



(b) Secondary compensation.

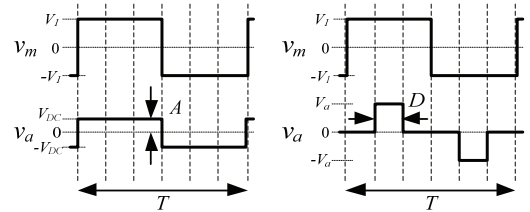
Fig. 3. Circuit diagrams of the proposed circuit.



(a) Step down chopper + Full bridge.

(b) Full bridge.

Fig. 4. Circuit diagrams of the auxiliary circuit.



(a) Step down chopper + Full bridge.

(b) Full bridge.

Fig. 5. Voltage waveforms of the proposed circuit.

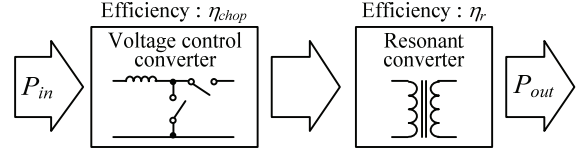


Fig. 1. Power flow diagram of the conventional circuit using a chopper circuit and a resonant converter.

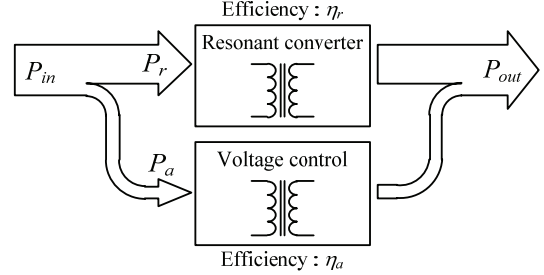


Fig. 2. Power flow diagram of the isolated DC/DC converter using the series voltage compensation.

proposed circuit  $f_0$  is obtained by (4) using the resonant capacitor  $C$  and the resonant inductance  $L$  that is containing the leakage inductance of the transformers.

$$f_0 = \frac{1}{2\pi\sqrt{LC}} \quad (4)$$

In addition, the auxiliary circuit can be connected to either primary side or secondary side of the main circuit as shown in Fig. 3. Fig. 3(a) shows the circuit configuration that the auxiliary circuit connects to the primary side. On the other hands, Fig. 3(b) shows a circuit configuration that the auxiliary circuit connects to the secondary side.

Fig. 4 shows the circuit configuration of the auxiliary circuit. Fig. 5 shows the voltage waveforms when the

auxiliary circuit is connected with the primary side.

Fig. 4(a) shows the circuit configuration which is the series connection of the step down chopper and full-bridge converter. In this circuit, the switching timing of the auxiliary circuit is synchronous with the main circuit. Then, the output voltage is controlled by changing the DC link voltage  $A$  between the step down chopper and full bridge converter. The high efficiency can be achieved by using the switching device with fast switching time for the step down chopper and low on-resistance for the full-bridge converter. However, the number of the switching device is increased.

Fig. 4(b) shows the full-bridge converter is used for the auxiliary circuit. In this circuit, the auxiliary circuit can output three different voltage levels;  $+V$ ,  $-V$ , and zero voltage. The output voltage is controlled by changing the pulse width  $D$  of the auxiliary circuit. The number of the switching device is decreased. However, the switching loss of the MOSFET is increased, and the control becomes complicated.

### III. MATHEMATICAL EXPRESSIONS OF POWER LOSS

This chapter explains the power loss expression of the proposed circuit. The power loss of the proposed circuit is separated into the main circuit side and auxiliary circuit. In the main circuit, the switching loss is ideally zero, because the main circuit FET can achieve ZCS periodically. Therefore, the power loss of the main circuit consists of the conduction loss and constant loss. The conduction loss is generated from the on-resistance of the FET, wire resistance of the transformer, and the equivalent series resistance of the capacitor. Likewise, the constant loss is generated within the iron-loss of the transformer, and no-load loss. On the other hand, the power loss of the auxiliary circuit consists of the conduction loss, constant loss, and switching loss, which are generated at the switching period, by the forward voltage drop of a switching device, respectively. It should be noted that the following mathematical expression is for the case of Fig. 3(a).

The resonant current of the proposed circuit is a sinusoidal waveform, provided that the resonant parameter of the proposed circuit is optimally designed. Therefore, the power loss per primary FET in the main circuit  $P_{loss\_FET\_main1}$  can be obtained by (5) using the on-resistance of the FET  $R_{on\_FET\_main1}$ .

$$P_{loss\_FET\_main1} = \frac{\pi^2}{8} R_{on\_FET\_main1} I_1^2 \quad (5)$$

The power loss of the auxiliary circuit FET consists of the conduction loss and switching loss. In the auxiliary circuit of Fig. 4(a), the conduction loss of the chopper FET  $P_{loss\_FET\_chop\_con}$  can be obtained by (6) using the on-resistance of the chopper FET  $R_{on\_chop}$  and the turn ratio of the transformer in the auxiliary circuit, which is  $\beta = N_{a1}/N_{a2}$ .

$$P_{loss\_FET\_chop\_con} = R_{on\_chop} (\beta I_1)^2 \quad (6)$$

In addition, the switching loss of the FET is proportional to the applied voltage and current. Therefore, the switching loss of the chopper  $P_{loss\_FET\_chop\_sw}$  is obtained by (7).

$$P_{loss\_FET\_chop\_sw} = V_1 (\beta I_1) (e_{on} + e_{off}) f_{sw} \quad (7)$$

where  $e_{on}$ [J] and  $e_{off}$ [J] are the turn-on and turn-off energy at per switching,  $f_{sw}$  is the switching frequency. In the full bridge converter, the switching loss is ideally zero, because the FET achieves ZCS. Therefore, the power loss per FET in the full bridge  $P_{loss\_FET\_FB}$  can be obtained by (8) using the on-resistance of the FET  $R_{on\_FET\_FB}$ .

$$P_{loss\_FET\_FB\_sw} = V_1 (\beta I_1) (e_{on} + e_{off}) f_{sw} \quad (8)$$

In the auxiliary circuit of Fig. 4(b), the conduction loss can be requested by expression (7) as well as the case of Fig. 4(a). The switching loss of the full-bridge converter is obtained by (9).

$$P_{loss\_FET\_FB\_sw} = \frac{\pi}{2} (\beta I_1) V_1 (e_{on} + e_{off}) f_{sw} \sin \left\{ \frac{\pi}{2} (1 - f_{sw} t_{on}) \right\} \quad (9)$$

where  $t_{on}$  is the compensation time per one cycle of the auxiliary circuit.

The power loss of transformer consists of the iron loss and copper loss. The iron loss occurs because of the flux changes in the core. The copper loss is occurring in the winding resistance of transformer. At first, when the square wave is inputted to the transformer, the flux density  $B_{ac}$  is obtained by (10).

$$B_{ac} = \frac{V_{N1} \cdot t_{on}}{2 N_1 A_c} \quad (10)$$

where  $V_{N1}$  is the primary voltage of the transformer,  $N_1$  is the primary wire turns,  $A_c$ [m<sup>2</sup>] is the effective cross-section of the core. Therefore, the iron loss of the transformer  $P_{trans\_fe}$  is obtained by (11) using the characteristics of the flux density - core loss value  $P_{cv}$ [W/m<sup>3</sup>] and the effective volume of the core  $V_e$ [m<sup>3</sup>].

$$P_{trans\_fe} = P_{cv} V_e \quad (11)$$

The copper loss of the transformer is obtained from the winding resistance with skin effect. The primary winding copper loss  $P_{loss\_Nm1}$  in the main circuit is obtained by (12) using the primary winding resistance of the main circuit with skin effect  $R_{N1\_main}$ . The transformer loss of the auxiliary circuit is obtained similarly.

$$P_{loss\_Nm1} = \frac{\pi^2}{8} R_{N1\_main} I_1^2 \quad (12)$$

The capacitor loss is obtained by the charge or discharge current of the capacitor and the equivalent series resistance of the capacitor. The resonant capacitor loss  $P_{loss\_C\_reso}$  is obtained by (13) using the equivalent series resistance  $R_{C\_reso}$ .

$$P_{loss\_C\_reso} = \frac{\pi^2}{8} R_{C\_reso} I_1^2 \quad (13)$$

The current based on the mean value of the sine wave is charged or discharged to the output capacitor. Therefore, the output capacitor loss  $P_{loss\_C\_out}$  is obtained by (14) using the equivalent series resistance  $R_{C\_out}$ .

$$P_{loss\_C\_out} = \left\{ \frac{\pi^2}{8} - 1 \right\} R_{C\_out} I_2^2 \quad (14)$$

#### IV. POWER LOSS CALCULATION

At first, the validity of the proposed calculation results is confirmed with the experimental results from the small type capacity prototype. The circuit configuration is a combination of the full-bridge converter with the secondary side compensation. (Fig. 3(b) and Fig. 4(b)).

Fig. 6 presents the efficiency of the proposed converter at a constant load when the primary voltage has a fluctuation of  $\pm 25\%$ . The secondary voltage is 12 V, the switching (resonant) frequency is 210 kHz, and the turn ratio of the main circuit transformer is  $N_1:N_2=4:2$ . Based on the input voltage characteristics, a maximum efficiency of 96.0% is obtained, when the input voltage is closed to the nominal input voltage. It should be noted that the synchronous rectification is applied to the secondary side in order to reduce the conduction losses of the rectifier. In addition, the experimental results and the calculation results are almost equivalent, especially, when the compensate voltage is small. On the other hand, when the compensate voltage is larger, the error margin of the loss becomes approximately 15% larger.

Fig. 7 shows the loss partition at  $P_{out}=100W$  and controlled by three different input voltage. From the result, the auxiliary FET loss increases in both the boost and buck modes, and the loss in the main circuit transformer are predominated.

Fig. 8 shows the primary current of the main transformer and the terminal voltage of  $S_{m2}$ . In both boost and step down mode accordingly, the main circuit is confirmed achieves zero current switching.

In the next section, four types of the auxiliary circuits shown in Fig. 3 and Fig. 4 are investigated and evaluated. The circuit parameters shown in Table 1 are used for calculation. The rating load is 2kW. The primary voltage has a fluctuation of  $48V \pm 25\%$ , and the secondary voltage has a fluctuation of  $380V \pm 25\%$ . Each of the primary side and secondary side compensate voltage by using the auxiliary circuit.

It should be noted that the voltage and the current value used for the calculation are ideal. Additionally, the resonant inductance, interconnection loss, and no-load loss are not included in the calculation loss.

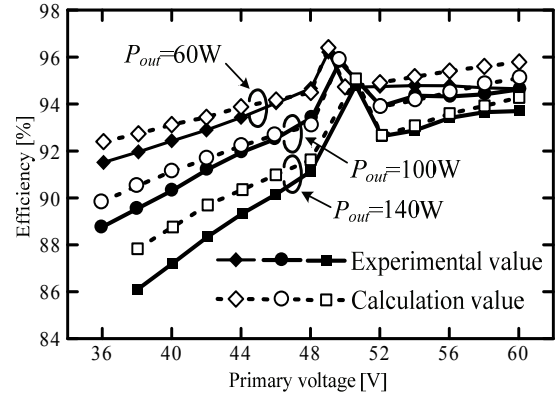


Fig. 6. Comparison between the experimental results and the calculation results by the prototype with small capacity. The circuit configuration is a combination of the full-bridge converter (Fig. 3(b)) with the output side compensation (Fig. 4(b)).

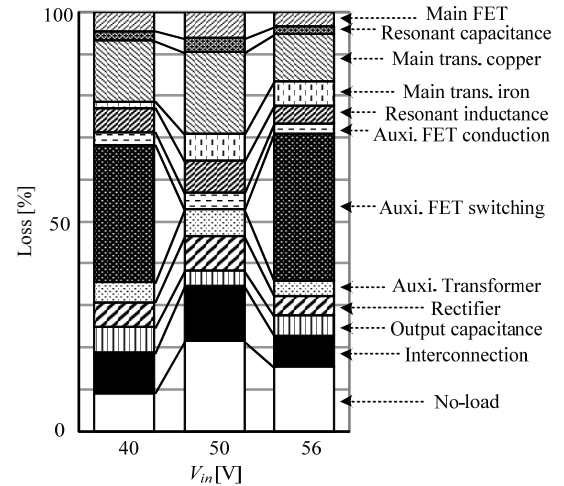


Fig. 7. Loss partition results of the calculation by the prototype with small capacity ( $P_{out}=100W$ )

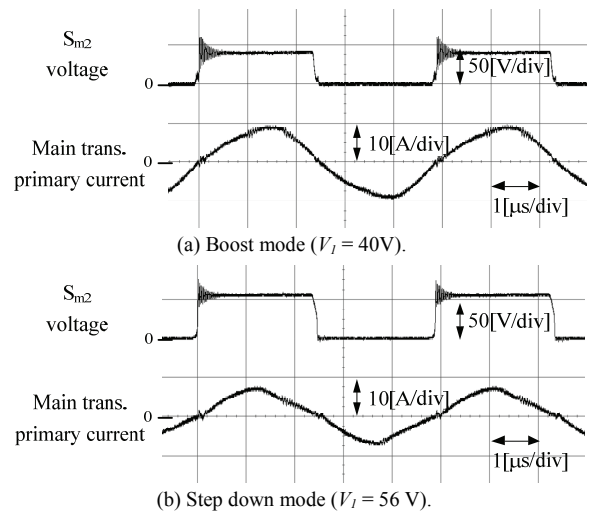
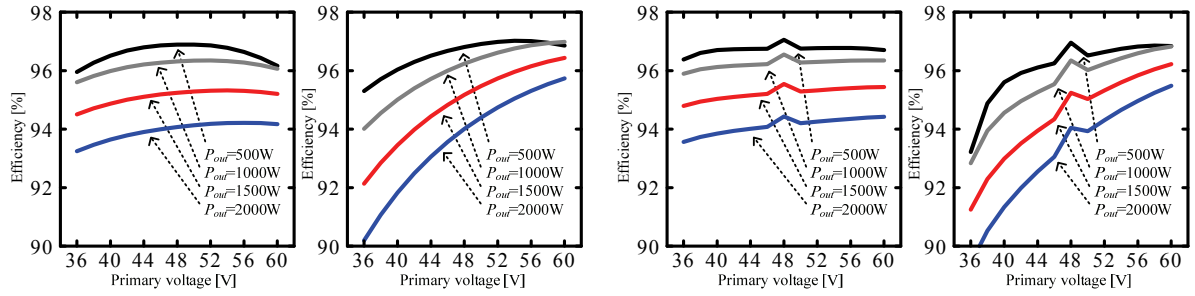
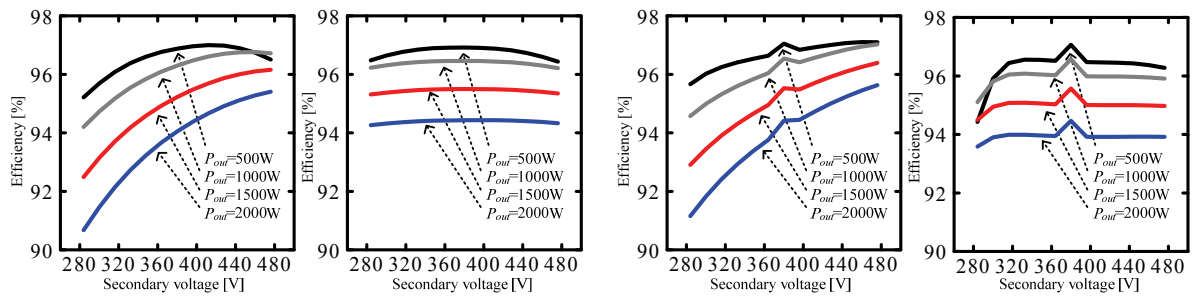


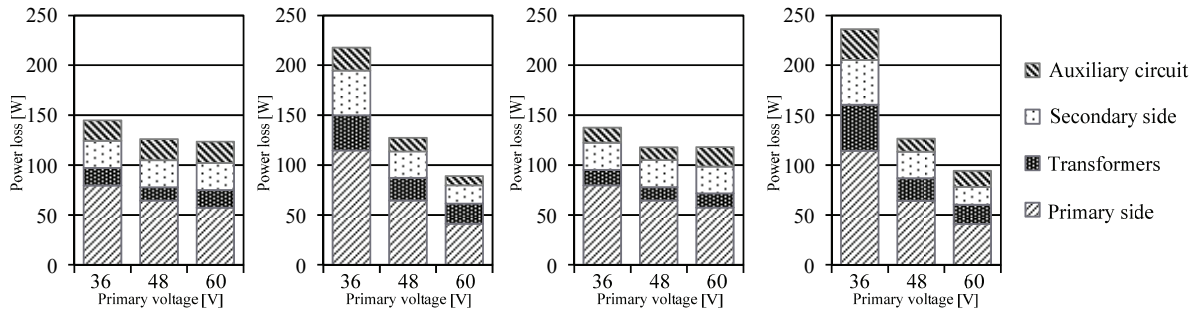
Fig. 8. Waveforms of the main transformer primary current and the terminal voltage of  $S_{m2}$  by the prototype with small capacity ( $P_{out}=100W$ ).



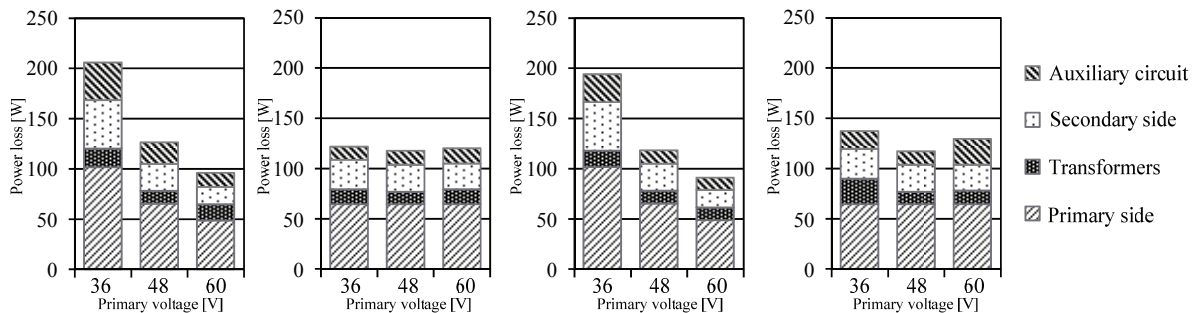
(a) Primary compensation. (b) Secondary compensation. (c) Primary compensation. (d) Secondary compensation.  
 Step down chopper + Full bridge. Step down chopper + Full bridge. Full bridge. Full bridge.  
 Fig. 9. Calculation results of the primary voltage compensation ( $V_1=48V\pm 25\%$ ,  $V_2=380V$ ).



(a) Primary compensation. (b) Secondary compensation. (c) Primary compensation. (d) Secondary compensation.  
 Step down chopper + Full bridge. Step down chopper + Full bridge. Full bridge. Full bridge.  
 Fig. 10. Calculation results of the secondary voltage compensation ( $V_1=48V$ ,  $V_2=380V\pm 25\%$ ).



(a) Primary compensation. (b) Secondary compensation. (c) Primary compensation. (d) Secondary compensation.  
 Step down chopper + FB. Step down chopper + FB. Full bridge. Full bridge.  
 Fig. 11. Power loss partition of the primary voltage compensation ( $V_1=48V\pm 25\%$ ,  $V_2=380V$ ,  $P=2000W$ ).



(a) Primary compensation. (b) Secondary compensation. (c) Primary compensation. (d) Secondary compensation.  
 Step down chopper + FB. Step down chopper + FB. Full bridge. Full bridge.  
 Fig. 12. Power loss partition of the secondary voltage compensation ( $V_1=48V$ ,  $V_2=380V\pm 25\%$ ,  $P=2000W$ ).

Table 1. Specification parameters of the power loss calculation for bi-directional isolated DC/DC converter.

Element	Symbol	Value
Input voltage	$V_1$	36 ~ 60 V (typ. 48 V)
Output voltage	$V_2$	284 ~ 476 V (typ. 380 V)
Rating power	$P_{out}$	2000 W
Switching frequency	$f_{sw}$	100 kHz
Wire turns (main trans.)	$N_{m1} : N_{m2}$	1 : 8
Wire turns (auxiliary trans.)	$N_{a1} : N_{a2}$	2 : 1

Fig. 9 presents the efficiency of the proposed converter at a constant load and a constant secondary voltage 48 V when the primary voltage has a fluctuation. Fig. 10 presents the efficiency of the proposed converter at a constant load and a constant primary voltage 380 V when the secondary voltage has a fluctuation.

In addition, Fig. 11 shows the power loss partition of the conditions in Fig. 8 ( $V_1 = 48V \pm 25\%$ ,  $V_2 = 380V$ ). Similarly, Fig. 12 shows the power loss partition on the conditions of Fig. 9 ( $V_1 = 48V$ ,  $V_2 = 380V \pm 25\%$ ).

From the loss calculation results, a maximum efficiency of 94.0 % is obtained in all the cases. Moreover, the high efficiency in a wide range can be achieved when the voltage fluctuation is compensated from the voltage changing side (ex. From the primary side when the primary side voltage changes (Fig. 9(a) and (c)), from the secondary side when the secondary side voltage changes (Fig. 9(b) and (d))). This is because, the efficiency reduces due to the difference in the power flow at the boost mode and buck mode. When the efficiency is decreased, the circulation current between the auxiliary circuit and the main circuit is increased. The efficiency is decreased when the voltage fluctuation is compensated from the voltage unchanging side (Fig. 9(b), (d) and Fig. 10(a), (c)). Therefore, the loss of the power circuit can be decreased when it connects the auxiliary circuit with the side of large voltage fluctuation side.

For example, the primary side is consisting of the large fluctuation voltage like the battery and the secondary side is low fluctuation range like the DC bus voltage, then, the power loss can be reduced by connecting the auxiliary circuit to the primary side.

Moreover, when the auxiliary circuit configuration is chopper + full-bridge, the conduction loss is increased. Therefore, to obtain the high efficiency, the auxiliary circuit is connected with a high voltage side. On the other hands, when the auxiliary circuit configuration is only full-bridge, the switching loss is increased. Therefore, to obtain high efficiency, the auxiliary circuit is connected at the low voltage side.

## V. EXPERIMENTAL RESULTS

The proposed converter was tested in the prototype to confirm the validity. It is considered that the proposed converter transfers energy between from battery to the DC bus. It is assumed that the primary side is connected to the battery. The battery voltage is 48 V, the one has fluctuation of  $\pm 25\%$ . And the secondary side is connected to the DC bus. The DC bus voltage is constant 380V.

The experimental circuit configuration is a combination of the full-bridge converter with the primary side compensation. (Fig. 3(a) and Fig. 4(b)). In this case, the battery voltage has large fluctuation. In addition, to obtain high efficiency, the auxiliary circuit is connected to the low voltage side.

At first, the experimental results of the main circuit are presented in order to confirm the high efficiency can be achieved in the main circuit. Then, experimental results of the proposed circuit are presented at the second.

### A. Experimental results of the main circuit

Fig. 12 shows the load characteristics of the main circuit. In this experiment, the auxiliary circuit is not operated. The power flow is from a primary side to a secondary side. The turn ratio of the transformer in the main circuit is 1:8. Therefore, the secondary voltage becomes 380V when the primary voltage of the main circuit is nearby 48V as shown in Fig. 12. However, the control method is an open-loop control,

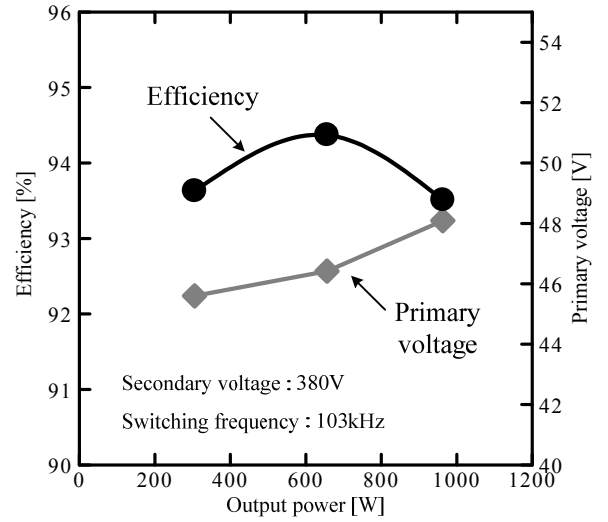


Fig. 12. Experimental results of the load characteristics only the main circuit (The auxiliary circuit is not operated).

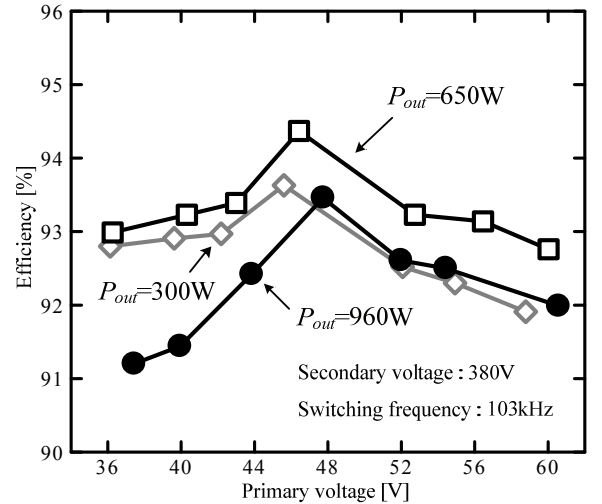


Fig. 13. Experimental results of the primary voltage compensation of the proposed circuit.

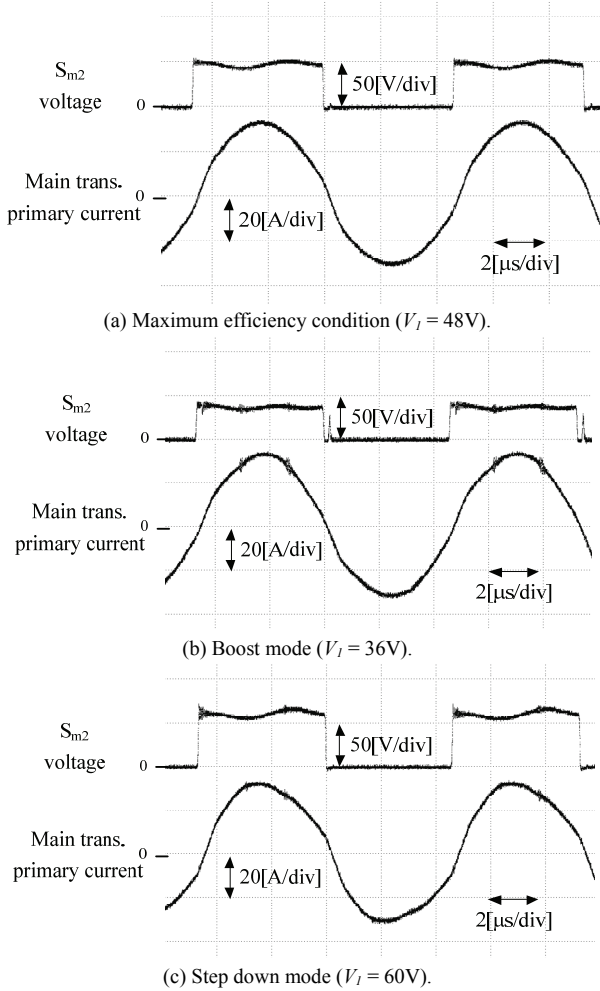


Fig. 14. Waveforms of the main transformer primary current and the terminal voltage of  $S_{m2}$  ( $P_{out}=960W$ ).

that is, the duty cycle is set to 50%.

As a result, the maximum efficiency of 94.5% is obtained at load of 650 W, as shown in Fig. 12. It is confirmed that the high efficiency is achieved in the main circuit.

### B. Experimental results of the proposed circuit

Fig. 13 presents the efficiency of the proposed converter at a constant load (380 V) when the primary voltage has fluctuation of  $\pm 25\%$ . In order to confirm the validity of the concept, the proposed converter was tested. The maximum efficiency of 94.5% is obtained, as shown in Fig. 13, when the primary voltage is closed to the nominal primary voltage (48 V). In both boost and step down modes, it was confirmed that the voltage control can be regulated while maintaining high efficiency.

Fig. 14 presents the primary current of the main transformer and the terminal voltage of  $S_{m2}$ . In the following orders, the maximum efficiency condition (The auxiliary circuit is not operated), and the boost and buck modes. Also, the full-bridge converter is controlled to achieve ZCS. A switching frequency is approximately 100 kHz was confirmed.

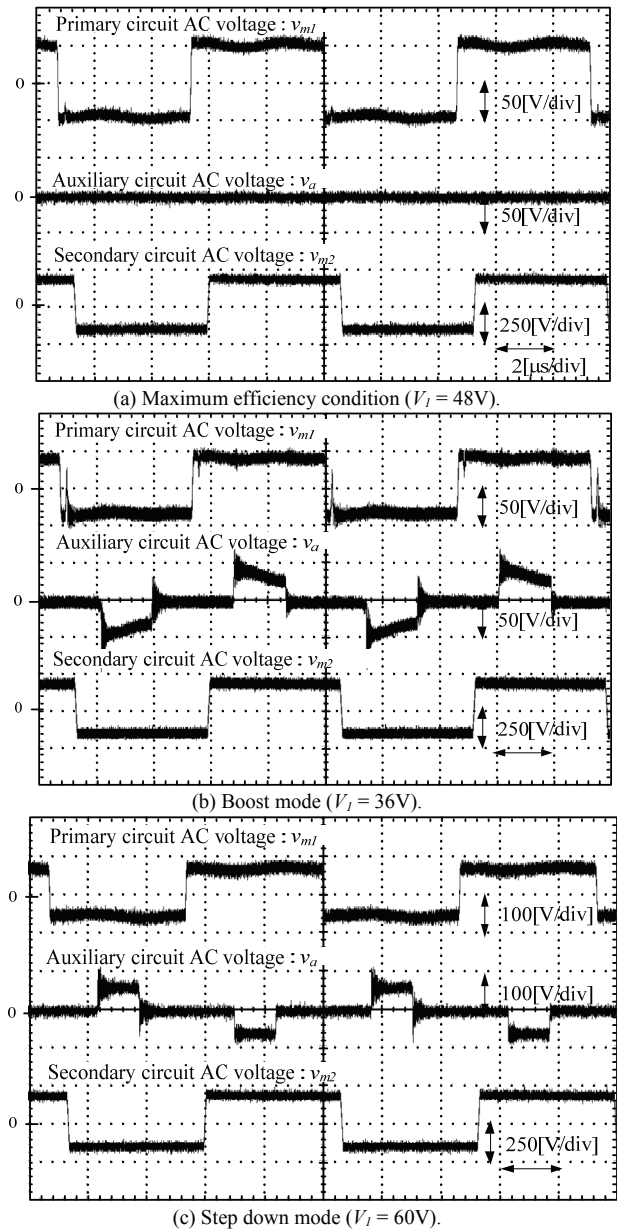


Fig. 15. AC voltage waveforms of the each circuit ( $P_{out}=960W$ ).

Fig. 15 presents the AC voltage waveforms of the each circuit. In both boost and step down modes, the auxiliary circuit outputs three different voltage levels;  $+V_1$ ,  $-V_2$ , and zero voltage. When the input voltage is decreased (Fig. 14(b)), the auxiliary circuit outputs a positive phase voltage to the main circuit without preventing the resonance operation of the main converter. Similarly, when the input voltage is increased (Fig. 14(c)), the auxiliary circuit outputs a negative phase voltage.

### C. Comparing of the calculation and experimental results

Since the experimental efficiency is lower than the expected efficiency, which from the calculation, as shown in Fig. 13 and Fig. 9(c). Therefore, in order to consider the causes of the difference between experimental results and expected results, the power loss of the experimental results was separated in detail.

Fig. 16 shows the loss partition of experimental efficiency for the maximum efficiency condition in Fig. 13. The experimental results and the calculation results are almost equivalent, as shown in Fig. 16. Even if the load conditions change, the error margin of the power loss becomes approximately 10%.

From the loss partition, the iron loss in the main transformer is predominant. This is because, the main transformer is evenly divided, and it is constructed by using two cores to increase the high boost up ratio. In the power loss calculation, only one core is considered for the main transformer. Additionally, the power loss of the resonant inductance is comprised 15% of the total loss. The resonant inductance loss is not included in the power loss calculation. If converter designs so that these losses become small, the efficiency of the proposed converter can be improved.

## VI. CONCLUSION

A series type bi-directional isolated DC/DC converter consisting of a current resonant type full-bridge converter and an auxiliary converter has been proposed. The concept of the series compensation is that the changing side voltage is regulated by adding or subtracting the auxiliary converter voltage to the current resonant type full-bridge voltage.

Four types of the auxiliary circuits are investigated and evaluated in term of losses. The relationship between the loss element and efficiency characteristics is clarified. The mathematical expression is established. The validity of the proposed circuit was confirmed by loss calculation, with a maximum efficiency of over 94% at 2kW.

The experimental results confirmed the maximum efficiency of 94.5% at 1kW is obtained when the primary voltage was closed to the nominal primary voltage. It was confirmed that the voltage control can be regulated while maintaining high efficiency. In addition, the experimental efficiency was lower than the expected efficiency was clarified by the loss separation.

In future work, the converter efficiency will be improved by the optimizing the design, the converter efficiency will be evaluated with a higher conversion capacity, and other circuit configuration patterns will be evaluated.

## REFERENCES

- [1] Krismer, F, Biela, J, Kolar, J. W. : "A comparative Evaluation of Isolated Bi-directional DC/DC Converters with Wide Input and Output Voltage Range", Industry Applications Conference 2005, pp.599-606, 2005.
- [2] S. Inoue, H. Akagi : "A Bi-directional DC/DC Converter for an Energy Storage System", Applied Power Electronics Conference, APEC 2007 - Twenty Second Annual IEEE., pp.761-767, 2007.
- [3] Du, Yu ; Lukic, Srdjan ; Jacobson, Boris ; Huang, Alex : "Review of high power isolated bi-directional DC-DC converters for PHEV/EV DC charging infrastructure", Energy Conversion Congress and Exposition (ECCE) 2011, pp.553-560, 2011
- [4] Wu, T.-F. ; Yang, J.-G. ; Kuo, C.-L. ; Lan, S.-Z. : "Isolated bi-directional full-bridge soft-switching dc-dc converter with active and passive snubbers", Applied Power Electronics Conference and Exposition (APEC) 2011, pp.844-850, 2011.
- [5] Aggeler, D. Biela, J. Inoue, S. Akagi, H. Kolar, J.W. : "Bi-Directional Isolated DC-DC Converter for Next-Generation Power Distribution - Comparison of Converters using Si and SiC Devices", Power Conversion Conference - Nagoya, 2007. pp.510-517, 2007.
- [6] J.Biela, U.Badstuebner, J.W.Kolar, "Impact of Power Density Maximization on Efficiency of DC-DC Converter Systems", IEEE Transaction on Power Electronics, Vol.24, No.1, pp.288-300, 2009.
- [7] K.Fathy, K.Morimoto, T.Doi, H.Ogiwara, H.W.Lee, M.Nakaoka, "A Diveded Voltage Half-Bridge High Frequency Soft-Switching PWM DC-DC Converter with High and Low Side DC Rail Active Edge Resonant Snubbers", IPEMC 2006, vol. 2, pp. 1-5, 2006.
- [8] Kheraluwala, M.N.; Gascoigne, R.W.; Divan, D.M.; Baumann, E.D. : "Performance characterization of a high-power dual active bridge DC-to-DC converter", Industry Applications, IEEE Transactions on Volume: 28, Issue: 6, pp.1294-1301, 1992.
- [9] Hui Li; Fang Zheng Peng; Lawler, J.S. : "A natural ZVS medium-power bidirectional DC-DC converter with minimum number of devices", Industry Applications, IEEE Transactions on Volume: 39, Issue: 2, pp.525-535, 2003.
- [10] M.Takagi, K.Shimizu, T.Zaitu, "Ultra High Efficiency of 95% for DC/DC Converter - Considering Theoretical Limitation of Efficiency", IEEE APEC 2002, vol. 2, pp. 735-741, 2002.
- [11] P.Alou, J.Oliver, J.A.Cobos, O.Garcia, J.Uceda, "Buck+half bridge (d=50%) topology applied to very low voltage power converters", APEC 2001, Sixteenth Annual IEEE Volume 2, pp 715-721, 2001.
- [12] S.Miyawaki, J.Itoh, K.Iwaya, "Optimization design of an Isolated DC/DC Converter Using Series Compensation on the Secondary Side ", ECCE 2010, pp1428-1435, 2010.

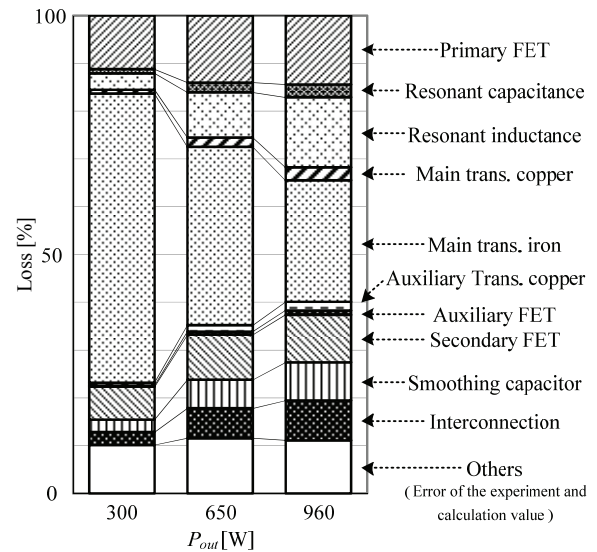


Fig. 16. Loss partition results of the calculation in maximum efficiency condition in Fig. 13